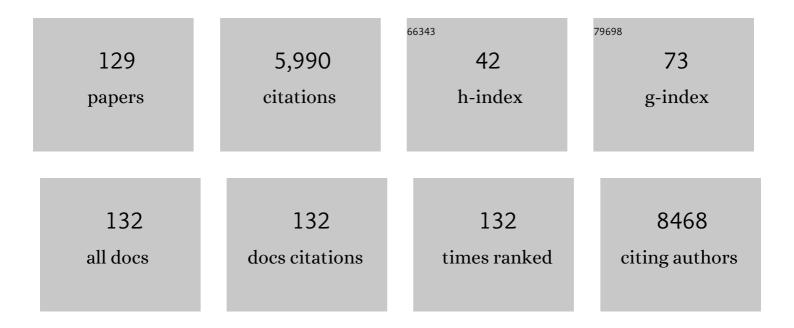
List of Publications by Year in descending order

Source: https://exaly.com/author-pdf/8721832/publications.pdf Version: 2024-02-01



#	Article	IF	CITATIONS
1	Highâ€performance holeâ€selective <scp>V<sub>2</sub>O<sub>X</sub></scp> / <scp>SiO<sub>X</sub></scp> / <scp>NiO<sub>X</sub></scp> contact for crystalline silicon solar cells. EcoMat, 2022, 4, .	11.9	15
2	Tunable work function of molybdenum oxynitride for electron-selective contact in crystalline silicon solar cells. Applied Physics Letters, 2022, 120, .	3.3	7
3	Heterostructure Silicon Solar Cells with Enhanced Power Conversion Efficiency Based on Si <sub><i>x</i></sub> /Ni <sup>3+</sup> Self-Doped NiO <sub><i>x</i></sub> Passivating Contact. ACS Omega, 2022, 7, 16494-16501.	3.5	17
4	Progress and Future Prospects of Wideâ€Bandgap Metalâ€Compoundâ€Based Passivating Contacts for Silicon Solar Cells. Advanced Materials, 2022, 34, e2200344.	21.0	30
5	Oneâ€Step Formation of Low Workâ€Function, Transparent and Conductive MgF <i><sub>x</sub></i> O <i><sub>y</sub></i> Electron Extraction for Silicon Solar Cells. Advanced Science, 2022, 9, .	11.2	17
6	Recent progress of metal-halide perovskite-based tandem solar cells. Materials Chemistry Frontiers, 2021, 5, 4538-4564.	5.9	15
7	Structural and optical studies of molybdenum oxides thin films obtained by thermal evaporation and atomic layer deposition methods for photovoltaic application. Journal of Materials Science: Materials in Electronics, 2021, 32, 3475-3486.	2.2	7
8	The rapidly reversible processes of activation and deactivation in amorphous silicon heterojunction solar cell under extensive light soaking. Journal of Materials Science: Materials in Electronics, 2021, 32, 4045-4052.	2.2	17
9	Surface Passivation of ITO on Heterojunction Solar Cells with Enhanced Cell Performance and Module Reliability. ECS Journal of Solid State Science and Technology, 2021, 10, 035008.	1.8	7
10	Phaseâ€Transitionâ€Induced VO <sub>2</sub> Thin Film IR Photodetector and Threshold Switching Selector for Optical Neural Network Applications. Advanced Electronic Materials, 2021, 7, 2001254.	5.1	27
11	Polarizable Highâ€Index Nanoparticles Used for Lightâ€Induced Crystalâ€Silicon Passivation and Dielectric Antenna for Highâ€Efficiency Solar Cell. Solar Rrl, 2021, 5, 2100169.	5.8	0
12	Post-annealing Effect on Optical and Electronic Properties of Thermally Evaporated MoOX Thin Films as Hole-Selective Contacts for p-Si Solar Cells. Nanoscale Research Letters, 2021, 16, 87.	5.7	14
13	Interfacial Engineering of Cu <sub>2</sub> O Passivating Contact for Efficient Crystalline Silicon Solar Cells with an Al <sub>2</sub> O <sub>3</sub> Passivation Layer. ACS Applied Materials & Interfaces, 2021, 13, 28415-28423.	8.0	25
14	Improved V <sub>2</sub> O <sub>X</sub> Passivating Contact for <i>p</i> â€Type Crystalline Silicon Solar Cells by Oxygen Vacancy Modulation with a SiO <sub>X</sub> Tunnel Layer. Advanced Materials Interfaces, 2021, 8, 2100989.	3.7	16
15	NiOx/MoOx bilayer as an efficient hole-selective contact in crystalline silicon solar cells. Cell Reports Physical Science, 2021, 2, 100684.	5.6	16
16	Bilayer MoO <sub><i>X</i></sub> /CrO <sub>X</sub> Passivating Contact Targeting Highly Stable Silicon Heterojunction Solar Cells. ACS Applied Materials & Interfaces, 2020, 12, 36778-36786.	8.0	28
17	Silicon Solar Cells: Stable MoO <i><sub>X</sub></i> â€Based Heterocontacts for <i>p</i> â€Type Crystalline Silicon Solar Cells Achieving 20% Efficiency (Adv. Funct. Mater. 49/2020). Advanced Functional Materials, 2020, 30, 2070325.	14.9	1
18	Stable MoO <i><sub>X</sub></i> â€Based Heterocontacts for <i>p</i> â€Type Crystalline Silicon Solar Cells Achieving 20% Efficiency. Advanced Functional Materials, 2020, 30, 2004367.	14.9	31

#	Article	IF	CITATIONS
19	Light Propagation in Flexible Thin-Film Amorphous Silicon Solar Cells with Nanotextured Metal Back Reflectors. ACS Applied Materials & Interfaces, 2020, 12, 26184-26192.	8.0	49
20	Substrate-free flexible thin film solar cells by graphene-mediated peel-off technology. Journal of Materials Science: Materials in Electronics, 2020, 31, 10279-10287.	2.2	1
21	Numerical study of mono-crystalline silicon solar cells with passivated emitter and rear contact configuration for the efficiency beyond 24% based on mass production technology. Journal of Semiconductors, 2020, 41, 062701.	3.7	11
22	Anisotropic performance of a superhydrophobic polyvinyl difluoride membrane with corrugated pattern in direct contact membrane distillation. Desalination, 2020, 481, 114363.	8.2	26
23	Thermoelectric properties of all-inorganic perovskite CsSnBr3: A combined experimental and theoretical study. Chemical Physics Letters, 2020, 754, 137637.	2.6	9
24	Interfacial Behavior and Stability Analysis of <i>p</i> â€Type Crystalline Silicon Solar Cells Based on Holeâ€Selective MoO <sub><i>X</i></sub> /Metal Contacts. Solar Rrl, 2019, 3, 1900274.	5.8	34
25	BiVO4 nanocrystals with controllable oxygen vacancies induced by Zn-doping coupled with graphene quantum dots for enhanced photoelectrochemical water splitting. Chemical Engineering Journal, 2019, 372, 399-407.	12.7	102
26	Impacts of alkaline on the defects property and crystallization kinetics in perovskite solar cells. Nature Communications, 2019, 10, 1112.	12.8	185
27	Interfacial Behavior and Stability Analysis of <i>p</i> â€Type Crystalline Silicon Solar Cells Based on Holeâ€ <del>S</del> elective MoO <sub><i>X</i></sub> /Metal Contacts. Solar Rrl, 2019, 3, 1970105.	5.8	11
28	Antireflective and self-cleaning glass with robust moth-eye surface nanostructures for photovoltaic utilization. Materials Research Bulletin, 2019, 109, 183-189.	5.2	36
29	Slippery for scaling resistance in membrane distillation: A novel porous micropillared superhydrophobic surface. Water Research, 2019, 155, 152-161.	11.3	183
30	High Weight-Specific Power Density of Thin-Film Amorphous Silicon Solar Cells on Graphene Papers. Nanoscale Research Letters, 2019, 14, 324.	5.7	5
31	Boosting Charge Separation and Transfer by Plasmon-Enhanced MoS <sub>2</sub> /BiVO <sub>4</sub> p–n Heterojunction Composite for Efficient Photoelectrochemical Water Splitting. ACS Sustainable Chemistry and Engineering, 2018, 6, 6378-6387.	6.7	77
32	High-Performance Dye-Sensitized Solar Cells Based on Colloid–Solution Deposition Planarized Fluorine-Doped Tin Oxide Substrates. ACS Applied Materials & Interfaces, 2018, 10, 15697-15703.	8.0	13
33	New-generation integrated devices based on dye-sensitized and perovskite solar cells. Energy and Environmental Science, 2018, 11, 476-526.	30.8	364
34	Phase-Separation-Induced PVDF/Graphene Coating on Fabrics toward Flexible Piezoelectric Sensors. ACS Applied Materials & Interfaces, 2018, 10, 30732-30740.	8.0	138
35	Flexible Asymmetric Supercapacitors Based on Nitrogenâ€Doped Graphene Hydrogels with Embedded Nickel Hydroxide Nanoplates. ChemSusChem, 2017, 10, 2301-2308.	6.8	37
36	Enhanced CMOS image sensor by flexible 3D nanocone anti-reflection film. Science Bulletin, 2017, 62, 130-135.	9.0	9

#	Article	IF	CITATIONS
37	Waferâ€Scale Highly Ordered Anodic Aluminum Oxide by Soft Nanoimprinting Lithography for Optoelectronics Light Management. Advanced Materials Interfaces, 2017, 4, 1601116.	3.7	27
38	Fast fabrication of TiO 2 hard stamps for nanoimprint lithography. Materials Research Bulletin, 2017, 90, 253-259.	5.2	18
39	Efficient and Flexible Thin Film Amorphous Silicon Solar Cells on Nanotextured Polymer Substrate Using Sol–gel Based Nanoimprinting Method. Advanced Functional Materials, 2017, 27, 1604720.	14.9	53
40	Improved growth rate of anodized TiO2 nanotube arrays under reduced pressure field and light illumination. Science Bulletin, 2017, 62, 332-338.	9.0	5
41	Reply to Comment on "Flexible Asymmetric Supercapacitors Based on Nitrogenâ€Doped Graphene Hydrogels with Embedded Nickel Hydroxide Nanoplates― ChemSusChem, 2017, 10, 2312-2315.	6.8	0
42	Scalable Production of Mechanically Robust Antireflection Film for Omnidirectional Enhanced Flexible Thin Film Solar Cells. Advanced Science, 2017, 4, 1700079.	11.2	13
43	Thin crystalline silicon with double-sided nano-hole array fabricated by soft UV-NIL and RIE. Materials Research Express, 2017, 4, 055005.	1.6	1
44	The effect of anions on the electrochemical properties of polyaniline for supercapacitors. Physical Chemistry Chemical Physics, 2017, 19, 14030-14041.	2.8	40
45	Microstructured superhydrophobic anti-reflection films for performance improvement of photovoltaic devices. Materials Research Bulletin, 2017, 91, 208-213.	5.2	30
46	Electrodeposition of polyaniline in long TiO2 nanotube arrays for high-areal capacitance supercapacitor electrodes. Journal of Solid State Electrochemistry, 2017, 21, 2349-2354.	2.5	14
47	Boosting electrocatalytic activities of plasmonic metallic nanostructures by tuning the kinetic pre-exponential factor. Journal of Catalysis, 2017, 354, 160-168.	6.2	14
48	Determination of the field strength and realization of the high-field anodization of aluminum. Physical Chemistry Chemical Physics, 2017, 19, 21696-21706.	2.8	11
49	Flexible broadband plasmonic absorber on moth-eye substrate. Materials Today Energy, 2017, 5, 181-186.	4.7	22
50	Derivation of a Mathematical Model for the Growth of Anodic TiO <sub>2</sub> Nanotubes under Constant Current Conditions. Journal of the Electrochemical Society, 2017, 164, E187-E193.	2.9	43
51	Tungsten based anisotropic metamaterial as an ultra-broadband absorber. Optical Materials Express, 2017, 7, 606.	3.0	65
52	Plasmonic Pd Nanoparticle- and Plasmonic Pd Nanorod-Decorated BiVO4 Electrodes with Enhanced Photoelectrochemical Water Splitting Efficiency Across Visible-NIR Region. Nanoscale Research Letters, 2016, 11, 283.	5.7	30
53	Periodic molybdenum disc array for light trapping in amorphous silicon layer. AIP Advances, 2016, 6, 055305.	1.3	2
54	Broad-band three dimensional nanocave ZnO thin film photodetectors enhanced by Au surface plasmon resonance. Nanoscale, 2016, 8, 8924-8930.	5.6	43

#	Article	IF	CITATIONS
55	Dual-Layer Nanostructured Flexible Thin-Film Amorphous Silicon Solar Cells with Enhanced Light Harvesting and Photoelectric Conversion Efficiency. ACS Applied Materials & Interfaces, 2016, 8, 10929-10936.	8.0	57
56	UV photodetectors based on 3D periodic Au-decorated nanocone ZnO films. Nanotechnology, 2016, 27, 365303.	2.6	15
57	Photoelectrochemical water splitting strongly enhanced in fast-grown ZnO nanotree and nanocluster structures. Journal of Materials Chemistry A, 2016, 4, 10203-10211.	10.3	67
58	Fabrication and supercapacitive performance of long anodic TiO 2 nanotube arrays using constant current anodization. Electrochemistry Communications, 2016, 68, 23-27.	4.7	50
59	3D periodic multiscale TiO <sub>2</sub> architecture: a platform decorated with graphene quantum dots for enhanced photoelectrochemical water splitting. Nanotechnology, 2016, 27, 115401.	2.6	52
60	High performance thin film solar cells on plastic substrates with nanostructure-enhanced flexibility. Nano Energy, 2016, 22, 539-547.	16.0	66
61	Enhancement of power conversion efficiency of dye sensitized solar cells by modifying mesoporous TiO2 photoanode with Al-doped TiO2 layer. Journal of Photochemistry and Photobiology A: Chemistry, 2016, 319-320, 62-69.	3.9	45
62	Valence Band Edge Shifts and Charge-transfer Dynamics in Li-Doped NiO Based p-type DSSCs. Electrochimica Acta, 2016, 188, 309-316.	5.2	37
63	Understanding the Enhancement Mechanisms of Surface Plasmonâ€Mediated Photoelectrochemical Electrodes: A Case Study on Au Nanoparticle Decorated TiO <sub>2</sub> Nanotubes. Advanced Materials Interfaces, 2015, 2, 1500169.	3.7	73
64	Highâ€Performance and Omnidirectional Thinâ€Film Amorphous Silicon Solar Cell Modules Achieved by 3D Geometry Design. Advanced Materials, 2015, 27, 6747-6752.	21.0	29
65	Silicon Solar Cells: Highâ€Performance and Omnidirectional Thinâ€Film Amorphous Silicon Solar Cell Modules Achieved by 3D Geometry Design (Adv. Mater. 42/2015). Advanced Materials, 2015, 27, 6768-6768.	21.0	5
66	Effects of acetyl acetone-typed co-adsorbents on the interface charge recombination in dye-sensitized solar cell photoanodes. Electrochimica Acta, 2015, 154, 190-196.	5.2	18
67	Inverted nanotaper-based Ag film for optical absorption and SERS applications. Journal of Alloys and Compounds, 2015, 632, 634-638.	5.5	13
68	Growth of anodic TiO2 nanotubes in mixed electrolytes and novel method to extend nanotube diameter. Electrochimica Acta, 2015, 160, 33-42.	5.2	31
69	The effect of Ni(CH3COO)2 post-treatment on the charge dynamics in p-type NiO dye-sensitized solar cells. Journal of Materials Science, 2015, 50, 6668-6676.	3.7	16
70	Effect of water content on ionic current, electronic current, and nanotube morphology in Ti anodizing process. Journal of Solid State Electrochemistry, 2015, 19, 1403-1409.	2.5	13
71	Theoretical derivation of anodizing current and comparison between fitted curves and measured curves under different conditions. Nanotechnology, 2015, 26, 145603.	2.6	83
72	Combined Au-plasmonic nanoparticles with mesoporous carbon material (CMK-3) for photocatalytic water splitting. Applied Physics Letters, 2015, 107, 073904.	3.3	7

#	Article	IF	CITATIONS
73	Influence of interface properties on charge density, band edge shifts and kinetics of the photoelectrochemical process in p-type NiO photocathodes. RSC Advances, 2015, 5, 71778-71784.	3.6	24
74	Highly Efficient Flexible Perovskite Solar Cells with Antireflection and Self-Cleaning Nanostructures. ACS Nano, 2015, 9, 10287-10295.	14.6	335
75	Quantitative relationship between nanotube length and anodizing current during constant current anodization. Electrochimica Acta, 2015, 180, 147-154.	5.2	48
76	Performance optimization of flexible a-Si:H solar cells with nanotextured plasmonic substrate by tuning the thickness of oxide spacer layer. Nano Energy, 2015, 11, 78-87.	16.0	31
77	Coupled optical and electrical modeling of thin-film amorphous silicon solar cells based on nanodent plasmonic substrates. Nano Energy, 2014, 8, 141-149.	16.0	24
78	Forming Process of Anodic TiO <sub>2</sub> Nanotubes under a Preformed Compact Surface Layer. Journal of the Electrochemical Society, 2014, 161, E135-E141.	2.9	72
79	High electro-catalytic counter electrode based on three-dimensional conductive grid for dye-sensitized solar cell. Chemical Engineering Journal, 2014, 255, 424-430.	12.7	16
80	Electropolymerization of Aniline onto Anodic WO <sub>3</sub> Film: An Approach to Extend Polyaniline Electroactivity Beyond pH 7. Journal of Physical Chemistry C, 2014, 118, 27449-27458.	3.1	42
81	Threeâ€Dimensional Structural Engineering for Energyâ€Storage Devices: From Microscope to Macroscope. ChemElectroChem, 2014, 1, 975-1002.	3.4	53
82	Morphology Defects Guided Pore Initiation during the Formation of Porous Anodic Alumina. ACS Applied Materials & Interfaces, 2014, 6, 2285-2291.	8.0	34
83	Flexible photovoltaic technologies. Journal of Materials Chemistry C, 2014, 2, 1233.	5.5	106
84	High-performance and renewable supercapacitors based on TiO2 nanotube array electrodes treated by an electrochemical doping approach. Electrochimica Acta, 2014, 116, 129-136.	5.2	252
85	Templated deposition of multiscale periodic metallic nanodot arrays with sub-10 nm gaps on rigid and flexible substrates. Nanotechnology, 2014, 25, 465303.	2.6	5
86	Simulation and Separation of Anodizing Current-Time Curves, Morphology Evolution of TiO2Nanotubes Anodized at Various Temperatures. Journal of the Electrochemical Society, 2014, 161, H891-H895.	2.9	15
87	Spatially controllable plasmon enhanced water splitting photocurrent in Au/TiO <sub>2</sub> –Fe <sub>2</sub> O <sub>3</sub> cocatalyst system. RSC Advances, 2014, 4, 45710-45714.	3.6	18
88	Large scale, flexible and three-dimensional quasi-ordered aluminum nanospikes for thin film photovoltaics with omnidirectional light trapping and optimized electrical design. Energy and Environmental Science, 2014, 7, 3611-3616.	30.8	43
89	Enhanced electroactivity at physiological pH for polyaniline in three-dimensional titanium oxide nanotube matrix. Physical Chemistry Chemical Physics, 2014, 16, 15796.	2.8	7
90	Enhanced Photoelectrochemical Water Splitting Performance of Anodic TiO <sub>2</sub> Nanotube Arrays by Surface Passivation. ACS Applied Materials & Interfaces, 2014, 6, 17053-17058.	8.0	107

#	Article	IF	CITATIONS
91	Light Management with Nanostructures for Optoelectronic Devices. Journal of Physical Chemistry Letters, 2014, 5, 1479-1495.	4.6	147
92	Fabrication of large diameter TiO 2 nanotubes for improved photoelectrochemical performance. Materials Research Bulletin, 2014, 60, 348-352.	5.2	15
93	Efficient suppression of nanograss during porous anodic TiO 2 nanotubes growth. Applied Surface Science, 2014, 314, 505-509.	6.1	24
94	Facile Method to Enhance the Adhesion of TiO <sub>2</sub> Nanotube Arrays to Ti Substrate. ACS Applied Materials & Interfaces, 2014, 6, 8001-8005.	8.0	138
95	Integrated Photoâ€supercapacitor Based on Biâ€polar TiO <sub>2</sub> Nanotube Arrays with Selective Oneâ€Side Plasmaâ€Assisted Hydrogenation. Advanced Functional Materials, 2014, 24, 1840-1846.	14.9	163
96	Inverted Nanocone-Based Thin Film Photovoltaics with Omnidirectionally Enhanced Performance. ACS Nano, 2014, 8, 6484-6490.	14.6	80
97	Roll-to-roll fabrication of large scale and regular arrays of three-dimensional nanospikes for high efficiency and flexible photovoltaics. Scientific Reports, 2014, 4, 4243.	3.3	71
98	Performance enhancement of thin-film amorphous silicon solar cells with low cost nanodent plasmonic substrates. Energy and Environmental Science, 2013, 6, 2965.	30.8	77
99	A simple route for decorating TiO2 nanoparticle over ZnO aggregates dye-sensitized solar cell. Chemical Engineering Journal, 2013, 229, 190-196.	12.7	35
100	Electrochemically hydrogenated TiO2 nanotubes with improved photoelectrochemical water splitting performance. Nanoscale Research Letters, 2013, 8, 391.	5.7	123
101	Enhanced supercapacitance in anodic TiO <sub>2</sub> nanotube films by hydrogen plasma treatment. Nanotechnology, 2013, 24, 455401.	2.6	127
102	SnO2@Si core–shell nanowire arrays on carbon cloth as a flexible anode for Li ion batteries. Journal of Materials Chemistry A, 2013, 1, 13433.	10.3	76
103	Improved electron-collection performance of dye sensitized solar cell based on three-dimensional conductive grid. Journal of Photochemistry and Photobiology A: Chemistry, 2013, 259, 10-16.	3.9	4
104	Molecular-scale interface engineering of metal nanoparticles for plasmon-enhanced dye sensitized solar cells. Dalton Transactions, 2013, 42, 5330.	3.3	23
105	Structural Engineering for High Energy and Voltage Output Supercapacitors. Chemistry - A European Journal, 2013, 19, 6451-6458.	3.3	22
106	Fabrication and Formation Mechanism of Triple-Layered TiO2Nanotubes. Journal of the Electrochemical Society, 2013, 160, E125-E129.	2.9	33
107	WE-C-103-03: Design of a Novel 3D Field Emission Electron Source for High Power X-Ray Tube. Medical Physics, 2013, 40, 481-481.	3.0	0
108	Flexible Dye-Sensitized Solar Cell Based on Vertical ZnO Nanowire Arrays. Nanoscale Research Letters, 2011, 6, 38.	5.7	38

#	Article	IF	CITATIONS
109	Quantum transport in indium nitride nanowires. Physical Review B, 2011, 83, .	3.2	12
110	Flexible Symmetric Supercapacitors Based on TiO\$_2\$ and Carbon Nanotubes. IEEE Nanotechnology Magazine, 2011, 10, 706-709.	2.0	21
111	Prototype of a scalable core–shell Cu2O/TiO2 solar cell. Chemical Physics Letters, 2011, 501, 446-450.	2.6	71
112	Temperature-dependent photoconductance of heavily doped ZnO nanowires. Nano Research, 2011, 4, 1110-1116.	10.4	14
113	Tunable wettability of metallic films with assistance of porous anodic aluminum oxide. Frontiers of Optoelectronics in China, 2010, 3, 317-320.	0.2	0
114	Formation of Anodic Aluminum Oxide with Serrated Nanochannels. Nano Letters, 2010, 10, 2766-2771.	9.1	106
115	Effects on Electronic Properties of Molecule Adsorption on CuO Surfaces and Nanowires. Journal of Physical Chemistry C, 2010, 114, 17120-17126.	3.1	115
116	Applications of Tunable TiO <sub>2</sub> Nanotubes as Nanotemplate and Photovoltaic Device. Chemistry of Materials, 2010, 22, 5707-5711.	6.7	74
117	Conductometric chemical sensor based on individual CuO nanowires. Nanotechnology, 2010, 21, 485502.	2.6	139
118	Piezoelectric PZT thick films on LaNiO <sub>3</sub> buffered stainless steel foils for flexible device applications. Journal Physics D: Applied Physics, 2009, 42, 025504.	2.8	10
119	Fabrication and magnetic behavior of chemical deposited Ni–P nanowire and nanotube arrays. Physica E: Low-Dimensional Systems and Nanostructures, 2009, 41, 349-352.	2.7	11
120	Self-Assembly of Periodic Serrated Nanostructures. Chemistry of Materials, 2009, 21, 253-258.	6.7	38
121	Weak Localization and Electronâ <sup>~</sup> 'Electron Interactions in Indium-Doped ZnO Nanowires. Nano Letters, 2009, 9, 3991-3995.	9.1	50
122	Templateâ€based Synthesis and Magnetic Properties of Cobalt Nanotube Arrays. Advanced Materials, 2008, 20, 4575-4578.	21.0	92
123	Investigation on highly ordered porous anodic alumina membranes formed by high electric field anodization. Materials Chemistry and Physics, 2008, 111, 168-171.	4.0	13
124	Fabrication of ZnO nanotubes with ultrathin wall by electrodeposition method. Materials Letters, 2008, 62, 3114-3116.	2.6	37
125	Fabrication of porous anodic alumina membranes with ultrathick barrier layer. Materials Letters, 2008, 62, 3228-3231.	2.6	8
126	Magnetic force microscopy observation of undercooled Fe <sub>81</sub> Ga <sub>19</sub> magnetostrictive alloys. Journal Physics D: Applied Physics, 2008, 41, 205405.	2.8	9

#	Article	IF	CITATIONS
127	The study on oxygen bubbles of anodic alumina based on high purity aluminum. Materials Letters, 2005, 59, 3160-3163.	2.6	43
128	Comparison of Energy Efficiency Between Fixed-speed and Variable-speed Wind Turbines. Energy Engineering: Journal of the Association of Energy Engineers, 2004, 101, 71-80.	0.5	3
129	Stable Molybdenum Nitride Contact for Efficient Silicon Solar Cells. Physica Status Solidi - Rapid Research Letters, 0, , 2100159.	2.4	8